CrystEngComm

Accepted Manuscript

ROYAL SOCIETY OF CHEMISTRY

www.rsc.org/crystengcomm

Journal Name

RSCPublishing

ARTICLE

Photoluminescent 3D lanthanide MOFs with a rare (10, 3)-*d* net based on a new tripodal organic linker

Cite this: DOI: 10.1039/x0xx00000x

Qing-Yuan Yang[a], Mei Pan[a,c]*, Shi-Chao Wei[a], Chien-Wei Hsu[b], Jean-Marie Lehn[b] and Cheng-Yong Su[a]*

Received 00th January 2012,
Accepted 00th January 2012

DOI: 10.1039/x0xx00000x

www.rsc.org/

A new semi-rigid tripodal ligand, namely, 1,1',1''-((2,4,6-triethylbenzene-1,3,5 triyl)tris(methylene))tris(pyridin-4(1H)-one) (**L1**), has been prepared by direct alkylation of 4-hydroxypyridine at the nitrogen site with 1,3,5-tris(bromomethyl)-2,4,6-triethylbenzene. The tripodal ligand has been used for the assembly of a series of isomorphous lanthanide metal–organic frameworks (Ln-MOFs) [Ln(**L1**)·$(NO_3)_3$]·nH_2O, (Ln = Eu (**1**), Tb (**2**), Sm (**3**), Ce (**4**), Gd (**5**); n = 3 or 4), which exhibit an unusual non-interpenetrated (10,3)-*d* (or **utp** net) topology. The photophysical properties of these lanthanide MOFs have been assessed, in which the Tb^{3+} complex **2** displays bright green luminescence with quite high efficiency ($\Phi_{overall}$ = 50 %) and long excited state lifetime (τ_{obs} = 1.1 ms).

Introduction

In the last decade, the design and construction of metal–organic frameworks (MOFs) has received great scientific attention, not only because of their intriguing architectures, but also due to their potential applications in gas sorption, molecular selection, heterogeneous catalysis and magnetic properties.[1, 2] One of remarkable features of MOFs that has recently triggered intense attention is the photoluminescent property.[3] Lanthanide-based luminescent MOFs have provided valuable platforms in many areas including biomedicine and solid state lighting.[4]

Lanthanide ions have unique character in exhibiting sharp and readily identifiable emission bands in both visible[5] and NIR regions.[6,7] However, due to their parity-forbidden nature, the absorption coefficients for f–f transitions are very low, which results in ineffective luminescence. Alternatively, the emission of the lanthanides can be sensitized by a coordinated ligand (antenna effect). In such case, excitation occurs at the singlet energy state of a suitable organic ligand, which subsequently relaxes to its triplet state and then transfers energy to the lanthanide ions.

The design of suitable antenna ligands is a vital factor for luminescent lanthanide metal–organic frameworks (Ln-MOFs). To achieve optimal luminescence quantum yields, the lowest excited triplet state ($^3\pi\pi^*$, or T_1) of a ligand should be slightly larger than the excited Ln-state (the energy difference represented as ΔE). Excited ligand states at lower energy than excited f-states of the Ln^{3+} ions do not allow energy transfer from the ligand to metal. The exact energy difference (ΔE) required for effective energy transfer involved in the antenna effect in Ln-MOFs is often of significant interest, although not easily elucidated. According to Latva's empirical rule,[8] the optimal ligand-to-metal transfer process for Eu^{3+} needs ΔE ($^3\pi\pi^*$-$^5D_0$) of ~2,500 cm^{-1}, and for Tb^{3+}, needs ΔE ($^3\pi\pi^*$-$^5D_4$) of ~2,000 cm^{-1}. Although the excited state $^4G_{5/2}$ of Sm^{3+} ion is at the level of 17,730 cm^{-1}, near to the $^5D_0$ state of Eu^{3+} (17,500 cm^{-1}), the sensitization of Sm^{3+} by antenna ligands is found difficult, and the relevant reports remain quite rare.[9] In comparison, the luminescence of Ce^{3+} ion is characteristic of parity-allowed electric-dipole 4f-5d transitions, which is quite different from the f-f transitions in Sm^{3+}, Eu^{3+} and Tb^{3+} complexes.[5b] Unfortunately, in most cases, the organic ligands could not well shield Ce^{3+} ion from luminescence quenching upon complexation. Nevertheless, the luminescence of the ligand can be reserved or modified in such cases, which found potential applications in many optical materials such as white-light modulation. We report herein a new type of Ln-MOFs based on a new tripodal antenna ligand, which can excite the emissions of Sm^{3+}, Eu^{3+} and Tb^{3+}, while remains its own blue emission in Ce^{3+}–MOF. Especially, the ligand has appropriate energy level for Tb^{3+}, which results in good energy transfer efficiency and high quantum yield.

Experimental

Materials and methods

Solvents were purchased from Sigma Aldrich and distilled from

appropriate drying agents prior to use. Commercially available reagents were used without further purification unless otherwise stated. NMR spectrum was recorded on Bruker Avance 400 NMR spectrometer. Absorption spectra were measured with a Jasco V-670 spectrophotometer. The powder X-ray diffraction (PXRD) data were recorded on a Bruker D8 ADVANCE X-ray powder diffractometer (Cu-Kα, λ = 1.5418 Å). The C, H, and N elemental analyses were performed on a Perkin-Elmer 240 elemental analyzer.

Photoluminescence spectra were taken at room temperature on a HORIBA Jobin-Yvon spectrometer. Emission and excitation spectra were corrected for source intensity (lamp and grating) by standard correction curves. Time-resolved measurements were performed using the multichannel scaling (MCS) single-photon-counting option on the HORIBA Jobin-Yvon IBHFL-322 Fluorolog 3. A pulsed xenon lamp was used to excite the sample. The excitation sources were mounted directly on the sample chamber at 90° to a double-grating emission monochromator and collected by a TBX-4-X single-photon-counting detector. The photons collected at the detector are correlated by a time-to-amplitude converter to the excitation pulse. Signals were collected using an IBH Data Station Hub photon-counting module, and data analysis was performed using the commercially available DAS6 software.

The quantum yield measurements were performed in quartz sample holder at appropriate excitation wavelength (the band maximum of excitation spectra), and collected emission wavelength from 400 nm to 850 nm using an absolute quantum yield measurement system (Hamamatsu, Model C11347-11).

Crystallography

Single-crystal reflection data were collected on an Oxford Gemini S Ultra diffractometer with the Enhance X-ray Source of Cu-Kα radiation (λ = 1.54178 Å) using the ω-φ scan technique. Empirical absorption correction was applied using spherical harmonics implemented in SCALE3 ABSPACK scaling algorithm. Structural solution and refinement against F^2 were carried out using the SHELXL programs. All the non-hydrogen atoms were refined with anisotropic parameters, while H atoms were placed in calculated positions and refined using a riding model, except for the H atoms of water molecules, which were found by electron cloud density (Q peaks). Crystallographic data and structural refinement information are listed in Table 1. The selected bond lengths and bond angles for compounds are listed in Table S1. Crystallographic data for the structures reported in this paper have been deposited with the Cambridge Crystallographic Data Centre as supplementary publication no. CCDC 979152 and 992360.

Synthesis of ligand

1,1',1''-((2,4,6-Triethylbenzene-1,3,5 triyl)tris(methylene))tris(pyridin-4(1H)-one) (L1): Under Ar, 1,3,5-tris(bromomethyl)-2,4,6-triethylbenzene (1.3 g, 3 mmol) was added to a suspension of 4-hydroxypyridine (0.95 g, 10 mmol) and K_2CO_3 (1.6 g, 12 mmol) in acetonitrile (30 ml). The reaction mixture was then refluxed at 83 °C for 24 h. On completion of the reaction, as indicated by TLC, the mixture was separated by filtration. The filtrate was evaporated at 40 °C under vacuum to give the crude product. The crude product was washed with acetone three times and dried under vacuum overnight. After that, **L1** was obtained as a white solid. Yield: 65 %. Melting point: 292 °C. ^{1}H-NMR (400 MHz, D_2O, 25 °C): δ = 2.58 (m, 6H, H_a), 0.80 (t, 9H, H_b), 5.34 (s, 6H, H_c), 6.44 (d, 6H, H_d), 7.59(d, 6H, H_e). MS (ESI$^+$, MeOH, *m/z*): calcd for $[M + H]^+$, 484.6; found, 484.8.

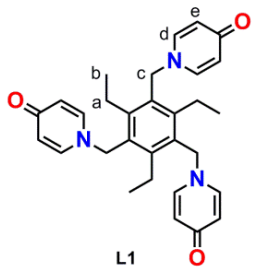

Scheme 1 Molecular structure of the ligand **L1**.

Synthesis of complexes

[Eu(L1)·(NO$_3$)$_3$]·3H$_2$O (1): A solution of **L1** (15 mg, 0.03 mmol) in water (2 ml) was added to a stirred solution of $Eu(NO_3)_3·6H_2O$ (9 mg, 0.02 mmol) in acetone (3 ml) at room temperature. The mixture was stirred for 30 min at room temperature. After filtration, slow diffusion of acetone into the filtrate over 7 days afforded colorless crystals. Yield: 58 %. Anal. Calc. (%) for $C_{30}H_{39}EuN_6O_{15}$: C, 41.15; H, 4.49; N, 9.60. Found: C, 40.84; H, 4.22; N, 9.49.

[Tb(L1)·(NO$_3$)$_3$]·4H$_2$O (2): Complex **2** was obtained by a similar procedure as for **1** except for using Tb $(NO_3)_3·6H_2O$ instead of Eu $(NO_3)_3·6H_2O$. Yield: 47 %. Anal. Calc. (%) for $C_{30}H_{41}N_6O_{16}Tb$: C, 40.01; H, 4.59; N, 9.33. Found: C, 40.18; H, 4.14; N, 8.98.

[Sm(L1)·(NO$_3$)$_3$]·4H$_2$O (3): Complex **3** was obtained by a similar procedure as for **1** except for using $Sm(NO_3)_3·6H_2O$ instead of $Eu(NO_3)_3·6H_2O$. Yield: 42 %. Anal. Calc. (%) for $C_{30}H_{41}N_6O_{16}Sm$: C, 40.39; H, 4.63; N, 9.42. Found: C, 40.17; H, 4.75; N, 9.16.

[Ce(L1)·(NO$_3$)$_3$]·3H$_2$O (4): Complex **4** was obtained by a similar procedure as for **1** except for using $Ce(NO_3)_3·6H_2O$ instead of $Eu(NO_3)_3·6H_2O$. Yield: 40 %. Anal. Calc. (%) for $C_{30}H_{39}CeN_6O_{15}$: C, 41.71; H, 4.55; N, 9.73. Found: C, 41.93; H, 4.82; N, 9.62.

[Gd(L1)·(NO$_3$)$_3$]·4H$_2$O (5): Complex **5** was obtained by a similar procedure as for **1** except for using $Gd(NO_3)_3·6H_2O$ instead of $Eu(NO_3)_3·6H_2O$. Yield: 53 %. Anal. Calc. (%) for $C_{30}H_{41}GdN_6O_{16}$: C, 40.08; H, 4.60; N, 9.35. Found: C, 40.43; H, 4.22; N, 9.07.

Results and discussion

The semi-rigid tripodal ligand **L1** as shown in Scheme 1 was prepared according to a slight modified literature procedure.[10] It should be noted that alkylation of 4-hydroxypyridine could produce *N*-substituted pyridones or *O*-substituted pyridines depending on the specific alkylating agent and conditions. For example, the *N*-

substituted pyridone occurs exclusively when α,α'-dibromo-o-xylene reacts with 4-hydroxypyridine,[11] but reactions with silyl chlorides produce only *O*-substituted pyridines.[12] However, alkylation with simple alkyl bromides could produce a mixture of *N*- and *O*-alkylation.[13] In this work, alkylation of 4-hydroxypyridine with 1,3,5-tris(bromomethyl)-2,4,6-triethylbenzene produces exclusively the *N*-substituted pyridine product as confirmed by NMR.

Table 1 Crystallographic data for complexes **2** and **4**.

	2	**4**
Formula	$C_{30}H_{41}N_6O_{16}Tb$	$C_{30}H_{39}CeN_6O_{15}$
F.w.	900.6	863.8
T (K)	150(2)	150(2)
Space group	$Pna2_1$ (No. 33)	$Pna2_1$ (No. 33)
a (Å)	15.091(1)	15.112(2)
b (Å)	16.736(1)	16.725(2)
c (Å)	13.071(1)	13.258(2)
α (°)	90	90
β (°)	90	90
γ (°)	90	90
V (Å^3)	3301.4(1)	3350.9(1)
Z	4	4
D_c (g cm^{-3})	1.703	1.641
μ (mm^{-1})	11.197	11.151
Data collected/unique	5838/3448	8885/4497
R_1 (>2/all data)	0.0297/0.0354	0.0289/0.0318
wR_2 (>2/all data)	0.0655/0.0666	0.0683/0.0692
GOF	1.052	0.997

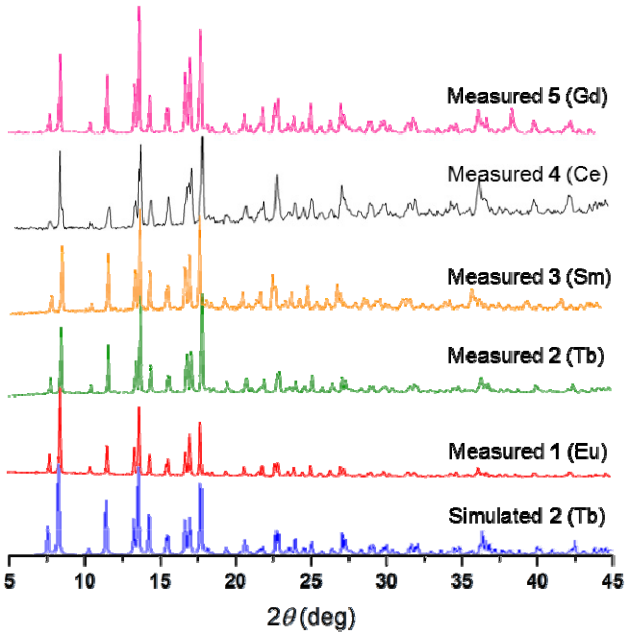

Fig. 1 The measured powder XRD patterns of complexes **1-5** in comparison to the simulated pattern of single-crystal **Tb-2**.

Reaction of **L1** with $Ln(NO_3)_3$ (Ln = Eu, Tb, Sm, Ce and Gd) resulted in complexes **1-5** respectively, namely $[Ln(\mathbf{L1})\cdot(NO_3)_3]\cdot nH_2O$ (Ln = Eu (**1**), Tb (**2**), Sm (**3**), Ce (**4**) and Gd (**5**); n = 3 or 4). After an initial exploration of the unit cells by preparatory single-crystal X-ray analyses, we found that the five complexes are isostructural. Furthermore, their phase purity and homogeneity were confirmed by powder X-ray diffraction as shown in Figure 1. As a consequence, only complexes **2** and **4** were chosen as representative compounds to collect the single-crystal reflection data. All complexes crystallize in the orthorhombic space group $Pna2_1$ and the asymmetric unit consists of one Ln^{3+}, one ligand **L1**, three coordinating NO_3^- anions and one water molecule. The Ln^{3+} ions lie in a tricapped trigonal prismatic geometry, bonded by three **L1** ligands through O atoms and three NO_3^- anions (Figure 2). Meanwhile, each tripodal ligand **L1** connects three Ln^{3+} ions, thus generating an intricate 3D framework as seen from Figure 3.

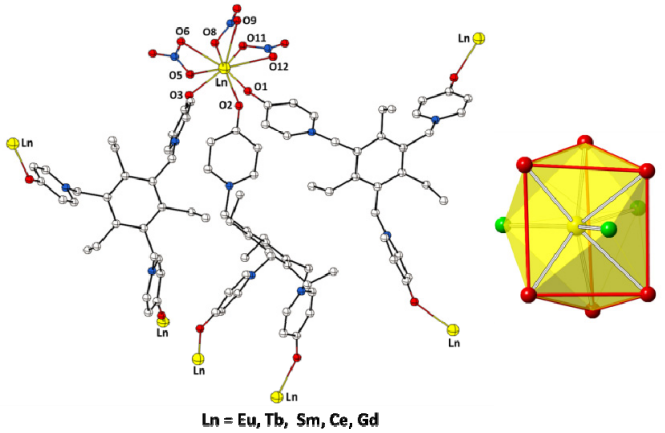

Fig. 2 Representative crystal structure showing coordination of central Ln^{3+} ion and surrounding ligands. The coordination geometry of Ln^{3+} is tricapped trigonal prismatic. The solvent molecules and hydrogen atoms are omitted for clarity.

A topological analysis of this 3D Ln-MOF was calculated by TOPOS 4.0.[14] If the coordinated NO_3^- anions are omitted, the Ln atoms can be looked at as a three-connected nonplanar node with triangular pyramidal geometry. Meanwhile, the tripodal ligand can be looked as a planar three-connected node. Therefore, the whole network can be represented topologically by two types of three connected nodes. One triangular-pyramidal node links three planar nodes and one planar node links three triangular-pyramidal nodes. The whole structure is extended into an unusual (10, 3)-*d* net [15] as displayed in Figures 3 and 4. The extended Schläfli symbol of this net is $10_2.10_4.10_4$, which is assigned to the **utp** net defined by O'Keeffe.[16] It should be noted that the (10,3)-*d* (or **utp**) net is rare compared to the common chiral (10,3)-*a* (srs) net, especially for non-interpenetrated ones. [17] Although this net resembles a (10,3)-*a* net in the sense that it has 4-fold helices, these helices are alternating left- and right-handed and the whole net is therefore racemic. To the best of our knowledge, there are only a few known coordination polymers showing (10, 3)-*d* topologies assigned in the papers.[17] Moreover, a lanthanide based coordination polymer with an **utp** net has not been reported to date. Therefore, the five isostructural networks described here constituted the first example of a coordination polymer network with a non-interpenetrated **utp** net constructed from lanthanide.

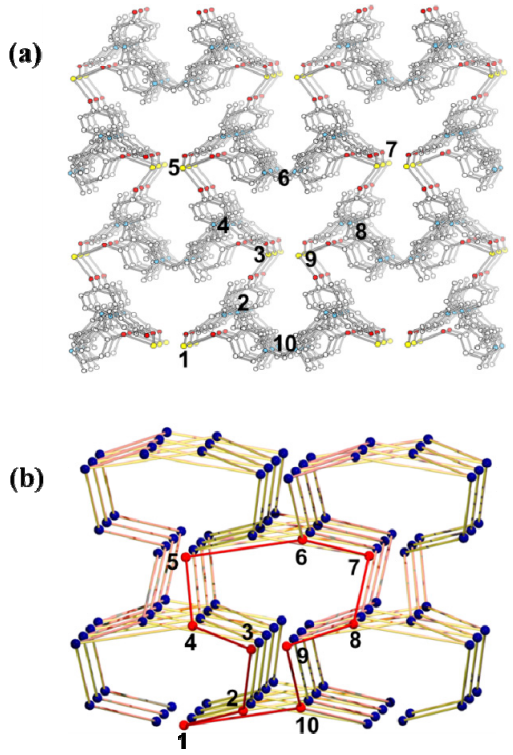

Fig. 3 (a) 3D Structure of the complexes along *a* axis with the solvent molecules, counter anions and hydrogen atoms omitted for clarity (yellow for Ln(III), blue for N, red for O, and white for C atoms, respectively). (b) The (10, 3)-*d* topological net, red line showing one 10-membered ring with numbers representating simplified nodes.

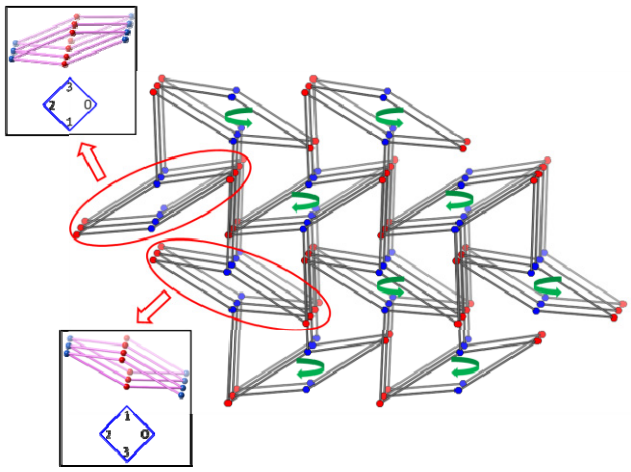

Fig. 4 View of the (10,3)-*d* topological net along *c*-axis and the alternating handedness of the 4-fold helices is shown.

As seen in Fig. 4, the **utp** net in these complexes possesses 4-fold helices along the *c* axis. Each helix is surrounded by six other adjacent helices that run through the crystal lattice to create channels. Because the right- and left-handed 4-fold helices are alternatively arranged, the whole net is therefore racemic. The present net is slightly distorted, because it contains two types of three connected nodes and cannot be classified as a regular net (in which all vertexes, edges, and angles are equivalent).

The luminescent properties of these complexes were investigated in the solid state. In agreement with the abundant literature dealing with lanthanide sensitization via ligand excitation,[18] particularly those with Eu^{3+} and Tb^{3+}, one of the main mechanisms of energy transfer involves the triplet states of the organic ligands. The energy of these states must be sufficiently tuned to maximize the energy transfer and minimize back-transfer processes.[19] Thus, the triplet energy level becomes an important issue when it comes to estimate the sensitization ability of an organic ligand. Since Gd^{3+} complex is structurally the same as Eu^{3+} and Tb^{3+}, it can provide information about ligand-centered (LC) electronic states because the Gd ($^6P_{7/2}$) level has too high energy to be populated by most known organic ligands. Moreover, due to the additional paramagnetic[20a] and heavy-atom[20b,c] effects produced by Gd^{3+} ion, both the ligand-based $^1\pi\pi^* \rightarrow {}^3\pi\pi^*$ intersystem crossing and $^3\pi\pi^* \rightarrow {}^1\pi\pi$ emission are increased, thus leading to strong $^3\pi\pi^* \rightarrow {}^1\pi\pi$ LC phosphorescence. Consequently, the complex [Gd(**L1**)·$(NO_3)_3$] (**5**) has been synthesized to determine the $^3\pi\pi^*$ triplet energy level of the **L1** ligand. The phosphorescence spectra of complex **5** were measured at 77 K as shown in Figure S1. The triplet state energy $^3\pi\pi^*$ of **L1** is estimated to be 22,727 cm^{-1}. It can be noted that the triplet energy level of the new tripodal ligand lies well above the energies of the main emitting levels of $^5D_0$ for Eu^{3+} (17 500 cm^{-1}), $^5D_4$ for Tb^{3+} (20 400 cm^{-1}) and $^4G_{5/2}$ of Sm^{3+} (17,730 cm^{-1}), therof suitable for sensitization of all these trivalent Ln^{3+} ions. Especially for Tb^{3+}, the energy difference ΔE ($^3\pi\pi^*$-$^5D_4$Tb) is near to the optimal 2000 cm^{-1}, thus making **L1** as an efficient antenna for the photosensitization of Tb^{3+} ion.[19a]

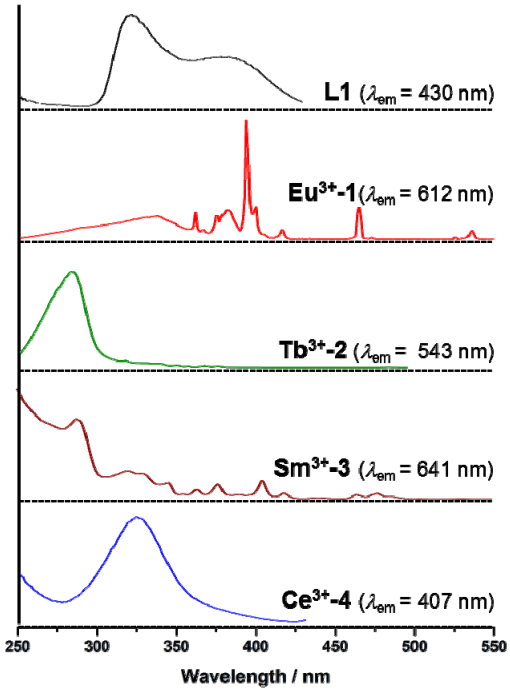

Fig. 5 Solid-state excitation spectra of ligand **L1** (top) and complexes [Ln(**L1**)·$(NO_3)_3$] with Ln = Eu, Tb, Sm, Ce (**1**, **2**, **3**, **4**) at room temperature.

The free ligand **L1** strongly absorbs UV irradiation via allowed π→π* transitions with band maximum centering at 37,736 cm^{-1} (265 nm, Fig. S2) in methanol solution. In the solid state, **L1** shows two apparent ππ*-related excitation bands centered at 320 and 360 nm, respectively. Excitation spectra of complexes **1-4** present broad bands in the range 250~400 nm owing to these ligand electronic transitions (Figure 5). Detailed analyses reveal that the excitation behaviors in the four Ln-MOFs are quite different. For **1** (Eu^{3+}) and **3** (Sm^{3+}), apart from the ligand-related excitation bands, additional peaks corresponding to the direct f-f transitions of Eu^{3+} or Sm^{3+} appeared. Especially, the intensity of $^7F_0 \rightarrow {}^5L_6$ (393 nm) and $^7F_0 \rightarrow {}^5D_2$ (460 nm) transitions of Eu^{3+} are much stronger than that of the ligand in complex **1**. This implies that direct energy transfer from the ligand to metal centeres via the antenna effect is not efficient enough for Eu^{3+} and Sm^{3+} complexes. In contrast, for Tb^{3+} complex (**2**), the excitation band was found to be remarkably predominant around 285 nm, which coincides well with the π→π* absorption of the free ligand **L1**. This observation indicates that, the energy transfer from the ligand to the Tb^{3+} centers in complex **2** is much more efficient than in Eu^{3+} and Sm^{3+} complexes. Consequently, the luminescent quantum yield of **2** is much higher (vide infra). Comparatively, the excitation spectra of Ce^{3+} complex (**4**) is more like that of the free ligand, although only one merged broad band centered at 323 nm was observed, indicative of metal-perturbing of the LC transitions.

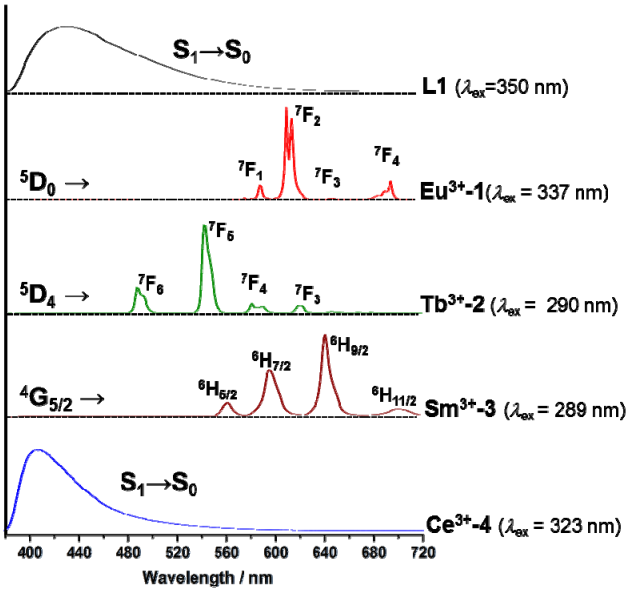

Fig. 6 Solid-state emission spectra of ligand **L1** (top) and complexes [Ln(**L1**)·$(NO_3)_3$] with Ln = Eu, Tb, Sm, Ce (**1**, **2**, **3**, **4**) at room temperature.

The emission spectra of the free ligand **L1** and the four complexes **1-4** in the solid state are shown in Figure 6. The ligand displays one broad emission peak centered at 430 nm. Under excitations into ligand excitation levels (280~350 nm), complexes **1-3** show the characteristic metal-centered luminescence of Eu^{3+}, Tb^{3+}, and Sm^{3+}, respectively. In the red luminescent complex **1**, narrow peaks originate from the transitions between Eu^{3+} lowest emitting state $^5D_0$ to $^7F_0$ (578 nm), $^7F_1$ (591 nm), $^7F_2$ (612~616 nm), $^7F_3$ (650 nm) and $^7F_4$ (688~700 nm) levels. The intensity of the $^5D_0 \rightarrow {}^7F_2$ (electric-dipole) transition is much stronger than that of the $^5D_0 \rightarrow {}^7F_1$ (magnetic-dipole) transition, indicating that Eu^{3+} ion has a low symmetric coordination environment without an inversion center, in agreement with the X-ray crystal analyses. Characteristically sharp and structured emission bands from Tb^{3+} cations are observed in complex **2**, which can be assigned to the $^5D_4 \rightarrow {}^7F_J$ (J = 6~3) transitions at 487 (J = 6), 542 (J = 5), 581-589 (J = 4), 620 (J = 3), 648 (J = 2), 669 (J = 1), and 678~681 nm (J = 0), respectively. In complex **3**, the narrow and sharp peaks from Sm^{3+} can be assigned to the $^4G_{2/5} \rightarrow {}^6H_J$ transitions at 561 (J = 5/2), 596 (J = 7/2), 641 (J = 9/2) and 702 (J = 11/2), respectively. In contrast, Ce^{3+} complex **(4)** shows blue luminescence with a broad band centered at 407 nm, comparable with the ligand-centered emissions and verified by the short lifetimes (τ = 0.8 and 4.3 ns) similar to that of ligand **L1** (τ = 0.8 and 3.2 ns). The ligand-centered emission bands at about 430 nm disappeared in the complexes **1-3**, implying that the energy migration from the ligand is complete, although the final sensitization efficiency of different Ln^{3+} centers is diverse.

Table 2 Life time (τ_{obs}) and overall quantum yields (Q_L^{Ln}) of the complexes.

compounds	τ_{obs} / μs	Q_L^{Ln}
Eu**L1**-(**1**)	779	0.06[a]
Tb**L1**-(**2**)	1100	0.50[b]
Sm**L1**-(**3**)	32	0.02[c]

[a] λ_{ex} = 337nm. [b] λ_{ex} = 290 nm. [c] λ_{ex} = 289 nm.

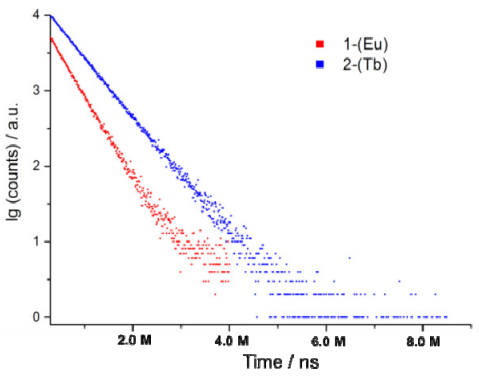

Fig. 7 The luminescent lifetime decay curves of complexes **1** and **2** monitored at 612 and 543 nm.

To further elucidate the metal-centered emission property, luminescence lifetimes and absolute luminescent quantum yields of complexes **1-3** have been measured (Table 2). Figure 7 illustrates the $^5D_0$ (Eu^{3+}) and $^5D_4$ (Tb^{3+}) decay curves measured at ambient (298 K) temperatures, which were monitored within the intense lines of the $^5D_0 \rightarrow {}^7F_2$ and $^5D_4 \rightarrow {}^7F_5$ transitions, respectively. In both cases, the observed luminescence decay profiles correspond to single exponential functions, thus confirming the presence of only one kind of emissive Eu^{3+} or Tb^{3+} centers in the crystal lattice. We can see quite long decay lifetimes in these two complexes, of which the Tb^{3+}

complex (τ_{obs}= 1.1 ms) obviously has even longer lifetime than the Eu^{3+} complex (τ_{obs}= 779 μs). This finding suggests that the ligand-to-lanthanide energy transfer for Tb^{3+} complex may be more effective than that for Eu^{3+} complex, which was also confirmed by the quantum yield values measured under ligand excitations. As seen from Table 2, the measured overall quantum yield (Q_L^{Ln}) of **2** is as high as 50%, significantly larger than those of Eu^{3+} (6%) and Sm^{3+} (2%). Such high quantum yields (Q_L^{Ln} ≥ 50%), although remain rare, have been previously obtained in other Tb^{3+} complexes.[21]

Based on above discussion, it is clear that, although the ligand **L1** can sensitize three Ln^{3+} ions, i.e. Tb^{3+}, Eu^{3+} and Sm^{3+}, the effectivity of the ligand-to-lanthanide energy transfer in these Ln^{3+} ions is evidently different. The overall sensitization efficiency (η_{sens}) of Eu^{3+} centers in complex **1** can be estimated according to the following equations:[22]

$$\eta_{sens} = \frac{Q_L^{Ln}}{Q_{Ln}^{Ln}} = Q_L^{Ln} \cdot \frac{\tau^{rad}}{\tau_{obs}} \quad (1)$$

$$\frac{1}{\tau^{rad}} = A_{MD,0} \cdot n^3 \left(\frac{I_{tot}}{I_{MD}}\right) \quad (2)$$

where Q_{Ln}^{Ln} represents the intrinsic quantum yield. From the emission spectrum of Eu^{3+} complex and the literature constant parameters, we calculated the η_{sens} value at only 12% for Eu^{3+} centers in complex **1**. In contrast, the η_{sens} value of Tb^{3+} in complex **2** is by no means less than 50% according to above equations. Since calculation of τ^{rad} for Tb^{3+} ion is not as straightforward as Eu^{3+} ion, thereof not readily available from present experimental data, it might be nonetheless informative to use the literature value (τ^{rad} = 1.9 ms) with comparable lifetime (τ_{obs}= 1.36 ms) for a rough estimation.[22a] As a result, the overall sensitization efficiency in complex **2** may reach η_{sens} = 86%, indicating that the ligand **L1** acts as an excellent sensitizer for Tb^{3+} luminescence.

Conclusions

We have demonstrated the first example of (10, 3)-*d* (or **utp**) net topology for Ln-MOFs. The new tripodal ligand can be used effectively as a three-connected node in conjunction with lanthanide nodes to produce a structurally consistent framework with this unusual topology. Furthermore, these new 3D Ln-MOFs are luminescent, displaying either metal-centered (red-Eu^{3+}, green-Tb^{3+} and redish-Sm^{3+}) or ligand-centered (blue for Ce^{3+}) emissions in the visible region. In this regard, the ligand **L1** represents a good candidate for preparing luminescent Ln-MOFs to achieve all three primary colors (red, green and blue) in one series of isostructural MOFs, offering the potential arena to build color-tunable or white-light emitting materials. Especially, a high quantum yield (50%) is obtained for the Tb^{3+} complex, indicating an efficient energy transfer thereof making the Tb-MOF as a promising green phosphor. Further studies on the applications of these luminescent Ln-MOFs are going in this laboratory.

Acknowledgements

This work was supported by the 973 Program of China (2012CB821701), the NSFC Projects (91222201, 21373276, 21121061, 21173272), the NSF of Guangdong Province (S2013030013474), the FRF for the Central Universities, and the RFDP of Higher Education of China for funding.

Notes and references

[a] MOE Laboratory of Bioinorganic and Synthetic Chemistry, State Key Laboratory of Optoelectronic Materials and Technologies, Lehn Institute of Functional Materials, School of Chemistry and Chemical Engineering, Sun Yat-Sen University, Guangzhou 510275, China
panm@mail.sysu.edu.cn; cesscy@mail.sysu.edu.cn

[b] Laboratoire de Chimie Supramoléculaire, Institut de Science et d'Ingénierie Supramoléculaires (ISIS), Université de Strasbourg, 8 allée Gaspard Monge, Strasbourg 67000, France

[c] State Key Laboratory of Structural Chemistry, Fujian Institute of Research on the Structure of Matter, Chinese Academy of Sciences, Fuzhou, Fujian 350002, PR China

Electronic Supplementary Information (ESI) available: [phosphorescence /absorption spectra and crystallographic information]. See DOI: 10.1039/b000000x/

1. (*a*) H. Furukawa, K. E. Cordova, M. O'Keeffe, O. M. Yaghi, *Science*, 2013, **341**, No. 6149, DOI: 10.1126/science.1230444; (*b*) H. C. Zhou, J. R. Long, O. M. Yaghi, *Chem. Rev*., 2012, **112**, 673; (*c*) C. Wang, D. M. Liu, W. B. Lin, *J. Am. Chem. Soc*., 2013, **135**, 13222; (*d*) Y. Liu, W. M. Xuan, Y. Cui, *Adv. Mater*., 2010, **22**, 4112; (*e*) S. M. Cohen, *Chem. Sci*., 2010, **1**, 32; (*f*) A. Dhakshinamoorthy, H. Garcia, *Chem. Soc. Rev*., 2012, **41**, 5262; (*g*) G. Férey, *Chem. Soc. Rev*., 2008, **37**, 191; (*h*) S. Horike, D. Umeyama, S. Kitagawa, *Acc. Chem. Res*., 2013, **46**, 2376.
2. (*a*) L. Q. Ma, J. M. Falkowski, C. Abney, W. B. Lin, *Nature Chemistry*, 2010, **2**, 838; (*b*) N. A. Vermeulen, O. Karagiaridi, A. A. Sarjeant, C. L. Stern, J. T. Hupp, O. K. Farha, J. F. Stoddart, *J. Am. Chem. Soc*., 2013, **135**, 14916; (*c*) R. B. Lin, F. Li, S. Y. Liu, X. L. Qi, J. P. Zhang, X. M. Chen, *Angew. Chem. Int. Ed*., 2013, **52**, 13429; (*d*) R. R. Yun, Z. Y. Lu, Y. Pan, X. Z. You, J. F. Bai, *Angew. Chem. Int. Ed*., 2013, **52**, 11282.
3. (*a*) Y. Cui, Y. Yue, G. Qian, B. Chen, *Chem. Rev*., 2012, **112**,1126; (*b*) M. D. Allendorf, C. A. Bauer, R. K. Bhakta, R. J. T. Houk, *Chem. Soc. Rev*., 2009, **38**, 1330; (*c*) J. Heine, K. Müller-Buschbaum, *Chem. Soc. Rev*., 2013, **42**, 9232; (*d*) K. Binnemans, *Chem. Rev*., 2009, **109**, 4283.
4. (*a*) S. V. Eliseevaa, J.-C. G. Bünzli, *Chem. Sci*., 2013, **4**, 1939; (*b*) Y. Li, S. Zhang, D. Song, *Angew. Chem., Int. Ed*., 2013, **52**, 710; (*c*) Y. L. Gai, K. C. Xiong, L. Chen, Y. Bu, X. J. Li, F. L. Jiang, M. C. Hong, *Inorg. Chem*., 2012, **51**, 13128.
5. (*a*) S. Petoud, S. M. Cohen, J.-C. G. Bunzli, K. N. Raymond, *J. Am. Chem. Soc.*, 2003, **125**, 13324; (*b*) X. L. Zheng, Y. Liu, M. Pan, X. Q. Lü, J. Y. Zhang, C. Y. Zhao, Y. X. Tong, C. Y. Su, *Angew. Chem., Int. Ed.*, 2007, **46**, 7399; (*c*) M. Pan, X. -L. Zheng, Y. Liu, W. -S. Liu, C. -Y. Su, *Dalton Trans.*, 2009, 2157.
6. (*a*) J. Zhang, P. D. Badger, S. J. Geib, S. Petoud, *Angew. Chem., Int. Ed.*, 2005, **44**, 2508; (*b*) J. An, C. M. Shade, D. A. Chengelis-Czegan, S. Petoud, N. L. Rosi, *J. Am. Chem. Soc.*, 2011, **133**, 1220.

7. (*a*) D. J. Lewis, P. B. Glover, M. C. Solomons, and Z. Pikramenou, *J. Am. Chem. Soc.*, 2011, **133**, 1033; (*b*) A. de Bettencourt-Dias, P. S. Barber, and S. Bauer, *J. Am. Chem. Soc.*, 2012, **134**, 6987; (*c*) L. D. Carlos, R. A. S. Ferreira, V. de Zea Bermudez, and S. J. L. Ribeiro, Adv. Mater. 2009, **21**, 509; (*d*) J. M. Stanley, B. J. Holliday, *Coordin. Chem. Rev.*, 2012, **256**, 1520.
8. M. Latva, H. Takalo, V.M.Mukkala, C.Matachescu, J. C. Rodriguez-Ubis and J. Kankare, *J. Lumin.*, 1997, **75**, 149.
9. (*a*) Z. Li, J. Yu, L. Zhou, H. Zhang, R. Deng, *Inorg. Chem. Commun.*, 2008, **11**, 1284; (*b*) S. Petoud, S. M. Cohen, J.-C. G. Bünzli, and K. N. Raymond, *J. Am. Chem. Soc.*, 2003, **125**, 13324; (*c*) H. Wang, S.-J. Liu, D. Tian, J.-M. Jia, and T.-L. Hu, *Cryst. Growth Des.*, 2012, **12**, 3263.
10. Q. Y. Yang, K. Li, J. Luo, M. Pan, C. Y. Su, *Chem. Commun*., 2011, **47**, 4234.
11. L. Johnson, Y. Kitahara, T. J. R. Weakley, J. F. W. Keana, *Tetrahedron Lett*., 1993, **34**, 5555.
12. H. Vorbrüggen, K. Krolikewwicz, *Chem. Ber*., 1984, **117**, 1523.
13. H. J. M. Dou, *J. Het. Chem.*, 1997, **14**, 321.
14. V. A. Blatov, *Struct. Chem*., 2012, **23**, 955.
15. V. A. Blatov, L. Carlucci, G. Cianib, D. M. Proserpio, *CrystEngComm*., 2004, **6**, 377.
16. M. O'Keeffe, *Reticular Chemistry Structure Resource*, see http://rcsr.anu.edu.au/nets/.
17. (*a*) H. Fu, Y. Lu, Z. L. Wang, C. Liang, Z. M. Zhang, E. B. Wang, *Dalton Trans*., 2012, **41**, 4084; (*b*) C. A. Black, L. R. Hanton, *Crystal Growth & Design*, 2007, **7**, 1868; (*c*) J. Zhang, Y. B. Chen, S. M. Chen, Z. J. Li, J. K. Cheng, Y.-G. Yao, *Inorg. Chem*., 2006, **45**, 3161; (*d*) J. R. Li, Q. Yu, E. C. Sanudo, Y. Tao, X. H. Bu, *Chem. Commun*., 2007, 2602; (*e*) J. Y. Sun, Y. M. Zhou, Z. X. Chen, G. S. Zhu, Q. R. Fang, R. J. Yang, S. L. Qiu, D. Y. Zhao, *J. Solid State Chem.*, 2006, **179**, 1230; (*f*) S. R. Halper, S. M. Cohen, *Inorg. Chem*., 2005, **44**, 486; (*g*) L. Öhrstrom, K. Larsson, S. Borg, S. T. Norberg, *Chem. Eur. J*., 2001, **7**, 4805; (*h*) Y. B. Dong, M. D. Smith, H. C. zur Loye, *Inorg. Chem*., 2000, **39**, 4927.
18. (*a*) E. G. Moore, A. P. S. Samuel, K. N. Raymond, *Acc. Chem. Res*., 2009, **42**, 542; (*b*) S. Petoud, *Chimia*, 2009, **63**, 745.
19. (*a*) S. V. Eliseeva, J.-C. G. Bünzli, *Chem. Soc. Rev*., 2010, **39**, 189; (*b*) J.-C. G. Bünzli, *Chem. Rev*., 2010, **110**, 2729; (*c*) J.-C. G. Bunzli, C. Piguet, *Chem. Soc. Rev*., 2005, **3**4, 1048.
20. (*a*) S. Tobita, M. Arakawa and I. Tanaka, *J. Phys. Chem*., 1985, **89**, 5649; (*b*) S. Tobita, M. Arakawa and I. Tanaka, *J. Phys. Chem*., 1984, **88**, 2697; (*c*) S. I. Klink, L. Grave, D. N. Reinhoudt, F. C. J. M. van Veggel, M. H. V. Werts, F. Geurts and J. W. Hofstraat, *J. Phys. Chem. A*, 2000, **104**, 5457.
21. (*a*) M. Seitz, E. G. Moore, A. J. Ingram, G. Muller, K. N. Raymond, *J. Am. Chem. Soc.*, 2007, **129**, 15468; (*b*) Z.-J. Lin, B. Xu, T.-F. Liu, M.-N. Cao, J. Lü, and R. Cao, *Eur. J. Inorg. Chem.*, 2010, 3842; (*c*) L. Ma, O. R. Evans, B. M. Foxman, W. B. Lin, *Inorg. Chem.*, 1999, **38**, 5837; (*d*) T. Fiedler, M. Hilder, P. C. Junk, U. H. Kynast, M. M. Lezhnina, M. Warzala, *Eur. J. Inorg. Chem.*, 2007, 291; (*e*) Q. L. Zhu, T. L. Sheng, R. B. Fu, S. M. Hu, J. S. Chen, S. C. Xiang, C. J. Shen, X. T. Wu, *Cryst. Growth Des.*, 2009, **9**, 5128.
22. (*a*) A. Aebischer, F. Gumy, J.-C. G. Bünzli, *Phys. Chem. Chem. Phys*. 2009, **11**, 1346; (*b*) M. V. López, S. V. Eliseeva, J. M. Blanco, G. Rama, M. R. Bermejo, M. E. Vázquez, and J.-C. G. Bünzli, *Eur. J. Inorg. Chem.*, 2010, 4532.

TOP Content

Isomorphous Ln-MOFs with rare (10,3)-*d* network were assembled from a dual functional ligand which sensitize Ln-based luminescence and achieve high quantum yield for Tb-MOF.